SSRG International Journal of Electrical and Electronics Engineering
ISSN: 2348-8379/ https://doi.org/10.14445/23488379/IJEEE-V10I7P114

Volume 10 Issue 7, 148-169, July 2023
© 2023 Seventh Sense Research Group®

Original Article

An Adaptive Ensemble Learning-Based Smart Face Recognition and Verification Framework with Improved Heuristic Approach

Santhosh Shivaprakash[1], Sannangi Viswaradhya Rajashekararadhya[2]

[1,2]*Department of Electronics and Communication Engineering, Kalpataru Institute of Technology, Tiptur,Tumkur District, Karnataka State, India.*

[1]*Corresponding Author : santhukit@gmail.com*

Received: 17 April 2023 Revised: 19 June 2023 Accepted: 08 July 2023 Published: 31 July 2023

Abstract *- Face recognition is an uncontrollable surveillance system but faces complex issues regarding minimal resolution, expression modification, and motion blur. Nowadays, researchers find more interest in face recognition analysis on pattern recognition and computer vision models. Several advancements in deep learning approaches for face recognition displayed a better efficacy rate in standard datasets. However, real-time face recognition approaches are applied and offer a poor efficacy rate. This modification leads to more changes in the testing and training set. Among these changes, misalignment of the face over testing and training effectively degrades the face recognition rate. Hence, resolving the abovementioned complications in the classical face recognition and verification technique is essential. Thus, a brand new face recognition and verification approach is developed based on optimal features and other approaches. Initially, images associated with face recognition are attained from the standard dataset and offered to pre-processing phase using median filtering. Then, the pre-processed images are fed to the feature extraction phase, the spatial features are acquired by Local Binary Pattern (LBP), and the spectral features are attained by 3 Discrete Wavelet Transform (3-DWT) levels. Later, the attained features are concatenated and utilized to obtain the optimal features by the Adaptive Crossover and Stallions Percentage-based Wild Horse Optimization (ACSP-WHO). Further, the attained optimal features are fed as the input to Ensemble Learning Network (ELNet)-based face recognition and verification phase, where the ensemble technique having Support Vector Machine (SVM), Deep Neural Networks (DNN), and Adaboost are utilized, and also the ACSP-WHO tunes their parameters to attain the practical face recognized and verified outcome in the developed model. Finally, the suggested face recognition and verification framework secured an effective efficacy rate than the traditional approaches in different experimental observations.*

Keywords *- Adaboost, Adaptive crossover, Stallions Percentage-based Wild Horse Optimization, Deep Neural Networks, Ensemble Learning Network, Face recognition and verification, Local Binary Pattern, Median filtering, Support Vector Machine, 3-level Discrete Wavelet Transform.*

1. Introduction

Recently, face recognition has been widely utilized to perform effective face identification in security analysis, personal identification, financial activities, and so on [10]. Face recognition utilizes three applications: face authentication, identification, and verification. Here, face recognition is utilized to detect a particular person in a dataset from more individuals [11]. Later, face verification is utilized to identify the correct person from two face images for resolving the different issues [12]. Further, face authentication is an issue verifying the face in facial authentication-based payment, phones, and wallets [13]. The face verification model recently gained more attention from commerce, transportation, and public safety professionals. In classical analysis, the acquired facial features, illuminations, expressions, and posture are essential for adequate face verification [14]. More analysis is performed for adequate face verification with many classes. In the unconstrained wild environment, face verifications performed by humans create more complications and are presented in the Labeled Faces in the Wild dataset [15]. The face image pairing performed for similar individuals presented in the database has multiple illuminations, expressions, and postures [16]. In this phase, the age difference among the individuals is slight, but the age difference in image pairs of various people is higher [17].

Moreover, the age factor generates more complications in the effectiveness of face verification. Also, ageing is termed a continuous natural and complicated process, which creates more changes in the human face regarding skin colour, wrinkles, and shape [18, 19]. In more practical applications, cross-age verification is determined as a unique application, and they are widely utilized in ID cards that are valid for nearly 20 years [20]. Thus, researchers decided to design an approach without considering the facial features but aimed to consider the difference in features based on age factor for a practical verification task [21].

This complexity issue falls in different aspects, such as the contrast in face pairs being varied in different ages. It contrasts in the same age being equal even if two face images are associated with various people [22]. Moreover, finally, the contrast in the face pair of huge age spans is more excessive than the minimal age span. So, designing an efficient cross-age-based face verification approach is a highly complicated issue [23].

The deep learning approach gained more interest in face verification and identification. Moreover, the deep learning approaches are classified into two classes: deep neural work-based models for acquiring discriminative and non-linear features [24]. Facial representation by employing DCNN is selected to perform effective face recognition. Here, DCNN effectively maps face image features with a normalization procedure [25].

Later, some of the multi-class classifiers are separated as multiple identities in the training set with a softmax classifier, and others learn the features with embedding models [26]. Followed by these existing works, a novel face recognition and verification framework is developed with machine learning and deep learning approaches [27, 28].

Multiple contributions to the recommended face recognition and verification framework are explained as follows.

- To design a novel face recognition and verification model with deep learning approaches to obtain effective face recognition and verification rate in real-world applications for executing automatic identification.
- To select essential features optimally using the developed ACSP-WHO for enhancing the efficacy rate in the recommended face recognition and verification framework.
- To implement a new ensemble-based face recognition and verification technique called ELNet to resolve the face identification complexities along with parameter optimization in SVM, DNN, and Adaboost with the recommended ACSP-WHO to maximize the accuracy of face recognition and verification.
- To initiate a novel heuristic framework called ACSP-WHO to optimize the degree and maximum iteration count in SVM, learning rate, and count of hidden neurons in DNN and estimator in Adaboost to effectively improve the efficacy rate of face recognition and verification.
- To validate the efficacy of the suggested face recognition and verification framework and different analysis over multiple verification models and algorithms.

The following stages of the recommended face recognition and verification framework are detailed. Existing research on face recognition and verification model is listed in Stage 2. The developed ensemble learning-based face recognition and verification technique with heuristic approaches is explained in Stage 3.

The concatenation of optimal features in the developed framework is analyzed in Stage 4. Structural views of the developed ensemble framework are presented in Stage 5. Various observations and their outcomes are explained in Stage 6, and the conclusion part is available in Stage 7.

2. Literature Survey

2.1. Related Works

In 2022, Deng et al. [1] suggested an Additive Angular Margin Loss (ArcFace) framework to attain crystal clear geographical interpretation and improve the discriminative power. The suggested ArcFace allowed more label noise; thus, sub-centerArcFacewas developed with K sub-centres. The sub-centerArcFace allowed the higher sub-classes to hold more clean face samples and the non-dominant class to utilize the noisy faces. The efficacies of the suggested model were improved by a self-propelled isolation model to clean the raw images in real-time noise. The recommended approach effectively provided the identity-preserved face image as the outcome with an improved discriminative feature than the traditional techniques.

In 2012, Zafeiriouet al. [2] developed a highly robust technique based on a discriminant kernel approach for adequate face verification and identification. Initially, Eigen observation was performed inside the scatter matrix directly presented in the search space. Moreover, the Eigen analysis offered Eigen spectrum in the range space based on their respective vector and null space. Kernel Discriminant Analysis (KDA) was fused in the developed model with the Eigen Spectrum Regularization model (ER-KDA). At last, the developed ER-KDA model was fused with a robust non-linear kernel for effective face identification and verification. The initiated framework was weighted with the prevalent approaches and secured a better efficacy rate than the classical models. In 2015, Krishnan and Naveen [3] initiated a facial verification and recognition framework with RGB-D data attained from the standard dataset named FRAV3D and Kinect. The FRAV3D dataset contained 106 subjects of men and women. Likewise, the Kinect dataset holds 17 images per 31 individuals. The developed models effectively validated the dataset with descriptor-based entropy. Some essential features were attained from a 2D face that was utilized as the input for the tree bagger classifier for attaining an efficient identity.

In 2023, authors [4, 5] recommended a face recognition model related to traits and features presented in the face due to the system being categorized as a biometric system. At first, improvements in the image were performed in the pre-processing phase, and then segmentation and reconstruction of the image were performed.

Next, the essential facial features were acquired and offered to perform better detection in face identification using wavelet transform and fractal model. Moreover, the LSTM structure was enhanced for training and testing in the developed framework. Finally, the suggested framework secured a better efficacy rate than the existing models.

In 2022, Asha et al. [6] introduced a more practical face recognition framework with a genetic approach to attain a reasonable search rate. The suggested models were classified into two phases: face pattern matching and face feature extraction. Here, the haralick features were attained from the face database with the PCA technique for efficient face recognition. Then, a swarm-based artificial firefly model was utilized to attain good search and match in the facial features. The recommended model secured a higher performance rate in the experimental observation than other techniques.

In 2020, Ni et al. [7] suggested a Multi-task related Deep Measure Learning model with a Boundary Discriminative Learning approach (MDML-BDL). It accurately analyzed the distance measures by investigating the discriminative data over the interclass neighbourhood samples like distance.

Moreover, the MDML-BDI effectively learned the non-linear transformation of non-linear data by fusing the metric learning in the multi-task deep neural network. Then, the other independent layers learned the transformation of a single particular task layer. Validation results showcased that the suggested technique secured a better efficacy rate than the classical observation throughout the analysis concerning Receiver Operating Characteristic (ROC) curve and accuracy.

In 2019, Ameuret al. [8] recommended an effectual feature retrieval scheme based on Gabor-based local binarized image features. Furthermore, a novel deep-structured architecture was utilized to acquire the essential features from the data processing component.

The technique was utilized for learning the multistage filter bank. Then, block histograms and binary hashing schemes were applied for pooling and indexing for efficient facial verification in the wild surrounding. At last, classification was executed with SVM and distance cosine and secured an effective efficacy rate than other techniques.

In 2020, Liu et al. [9] proposed a new model based on the unconstraint surveillance task in face recognition. Initially, Generative Adversarial Network (GAN)-based approach was utilized to attain the highly robust feature from the raw surveillance frames, effectively improving recognition accuracy and minimizing the validation cost in face matching. Then, enhanced center loss functions were fused with unlabeled surveillance faces to accurately classify the identities in the developed framework. In the recommended model, the discriminative rate was improved efficiently and verified with two standard datasets.

2.2. Problem Statement

Face recognition is a complicated issue when face images are not aligned accurately. Because the face images are attained from different angles, they are not accurately cropped by automatic approach or humans. Several complications presented in the classical face recognition and verification models are displayed in Table 1.

ArcFace [1] effectively enhances the discriminative power and the generative power. Moreover, it needs to enhance the privacy rate. KDA [2] has a better robustness rate, is easy to implement, and is faster. However, it always needs average distribution assumptions to predict the essential features. Random forest [3] has a high-reliability rate and offers a better outcome rate in utilizing a small dataset. However, it needs a considerable training dataset per subject and does not support a large dataset. MPM-LSTM [4] effectively analyzes imperfect facial data and processes the data faster and more accurately.

However, it did not utilize small data for the analysis and faced vanishing gradient issues. PCA [6] effectively minimizes the issues related to overfitting, enhances the visualization rate, and neglects the correlated features. Still, it needs to resolve the information loss issues during analysis, and also it is complex to analyze due to the presence of a covariance matrix. MDML-BDI [7] attains a better efficacy rate in terms of accuracy and ROC curve. However, it suffers a lot when large datasets are offered.

WPCA [8] has a minimal time consumption rate, offers an effective accuracy rate, and effectively minimizes the noise in the data. Still, it has a minimal interpretability rate and needs to resolve the sensitivity issue. PA-GAN [9] effectively reduces the computational cost, enhances the accuracy rate, and accurately classifies the identities. However, it is unstable and complicated to train effectively, requiring more time for practical analysis. Different complexities presented in the existing approaches are required to resolve; thus, novel face recognition and verification models with multiple approaches are developed.

Table 1. Features and challenges of existing face recognition and verification framework with different techniques

Author [Citation]	Techniques	Advancements	Complexities
Deng et al. [1]	ArcFace	• It effectively enhances the discriminative power and the generative power.	• It needs to enhance the privacy rate.
Zafeiriouet al. [2]	KDA	• It has a better robustness rate. • It is easy to implement, and they are faster.	• It always needs standard distribution assumptions to predict the essential features.
Krishnan and Naveen [3]	Random forest	• It has a high-reliability rate. • It offers a better outcome rate in the utilization of a small dataset.	• It needs a considerable training dataset per subject and does not support a large dataset.
Mahmood and Kurnaz [4]	MPM-LSTM	• It effectively analyzes imperfect facial data. • It processes the data faster and more accurately.	• It did not utilize small data for the analysis. • It faces a vanishing gradient issue.
Asha et al. [6]	PCA	• It effectively minimizes the overfitting issue and also enhances the visualization rate. • It neglects the correlated features.	• It needs to resolve the information loss issues during analysis. • It is complex to analyze due to the presence of a covariance matrix.
Ni et al. [7]	MDML-BDI	• It attains a better efficacy rate in terms of accuracy and ROC curve.	• It suffers a lot when large datasets are offered.
Ameuret al. [8]	WPCA	• It has a minimal time consumption rate and an effective accuracy rate. • It effectively minimizes the noise presented in the data.	• It has a minimal interpretability rate and needs to resolve the sensitivity issue.
Liu et al. [9]	PA-GAN	• It effectively reduces the computational cost and also enhances the rate of accuracy. • It accurately classifies the identities.	• It is unstable and complicated to train effectively. • It needs more time for the analysis.

3. Integration of Ensemble Learning-Based Face Recognition and Verification Framework with Enhanced Heuristic Mechanism

3.1. Developed Ensemble-Based Face Recognition and Verification Model

The need for highly reliable personal identification in computer-based access control increased the researcher's interest in developing biometrics for replacing ID cards and passwords, as passwords and ID cards are breached and easily attacked by unauthorized users. Biometrics utilizes human features like a dynamic signature, fingerprint, iris, face, speech, and retinato to verify individuals' identities. The data associated with biometrics are kept safe, and they cannot steal or share easily. The face identification model offered more benefits to the user by verifying the personal identity in a non-intrusive and passive system. Most of the existing face recognition and identification system utilizes face identification, face detection, and face authentication.

In the verification process, the system previously knows the user's identity and verifies whether the user is an attacker. However, in face recognition, the user's identity is not known previously, and the system needs to decide by analyzing the existing images. Most of the researchers utilized a machine-learning approach for effective verification outcomes. However, these face verification approaches are widely suffered from occluded images with more obstacles, scarf, and maskson the face. Thus, to resolve the complications presented in the face recognition and verification approach, a novel face verification approach is developed with ensemble learning models, and it is presented in Fig. 1.

A brand new face recognition and verification framework is developed based on ensemble approaches to attain effective face recognition and face recognition rates among individuals. At first, essential data employed for the observation are gathered from two standard datasets and subjected as the input to pre-processing phase. Here, the original images are pre-processed by a median filtering scheme. Then, the pre-processed images are forwarded to the feature extraction region. Here, two different features, spatial and spectral features, are acquired, where spatial features are attained using LBP, and three levels of DWT acquire the spectral features. Further, the attained spatial features from LBP and spectral features from 3-DWT are offered to the features concatenation phase. Then, the obtained concatenated features are utilized to attain the optimal features by developing ACSP-WHO. Later, the acquired optimal features are provided as the input to ELNet, consisting of different techniques like SVM, DNN, and Adaboost.ACSP-WHO tunes its parameters by maximizing the accuracy of verification—finally, the face-recognized and verified outcomes are attained by averaging the SVM, DNN, and Adaboost scores.

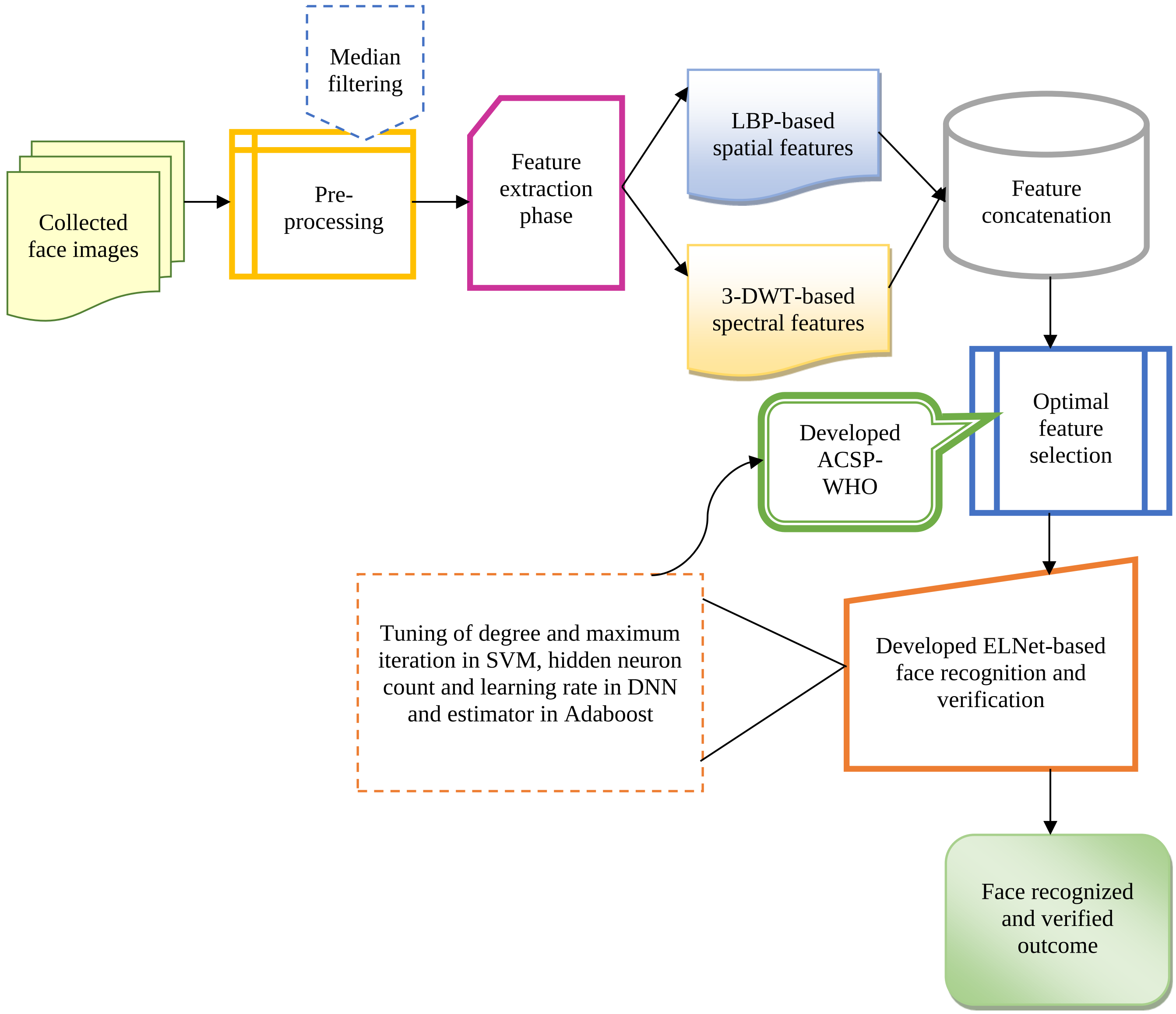

Fig. 1 Pictorial representation of face recognition and verification framework

3.2. Experimental Face Image Dataset

Different images utilized for practical face recognition and verification analysis are attained from two standard datasets, elaborated below.

Dataset 1-Yale Dataset: The essential analysis images are collected from the link: "http://vision.ucsd.edu/content/yale-face-database: Access Date: 2023-02-18". The dataset holds nearly 165 images of 15 people with facial expressions like sleepy, right-light with glasses, sad, without glasses, wink, happy, left-light, surprised, centre-light, and normal.

Dataset 2-CFPW: This dataset holds celebrities' images in frontal-profile view format. It has four different profiles along with ten frontal images of 500 individuals.

The data are collected from the link: "http://www.cfpw.io/: Access Date: 2023-02-19". The sample images gathered from the dataset are displayed in Figure 2.

The attained face images for the analysis are termedIM^a_q where, q = 1, 2, 3,….Q and B indicate the pre-processed image count.

4. Optimal Feature Concatenation for Ensemble-based Face Recognition and Verification Model

4.1. Face Image Pre-Processing

The acquired images IM_q^a and utilized as the input to the pre-processing image phase. Here, the median filtering approach performs effective pre-processing in the original image. Median filtering [30] is a non-linear-related filtering model that effectually reduces the noise in the original images. This median filtering approach mainly focused on preserving the edges of the image to reduce the error during processing. It is a highly robust filter and performs averaging in the adjacent filters. In the developed face recognition and verification model, median filtering effectively enhances the image quality, and the median value of the image is offered in Eq. (1).

$$MED\left(IM_q^a\right) = \begin{cases} IM_{P+1} = IM_u & Q = 2p+1 \\ \frac{1}{2}\left(IM_{P+1} + IM_p\right) & Q = 2p \end{cases} \tag{1}$$

The median ranks in the image are presented as $u = IM_{p+1}$ and also the 2-D median filtering utilized to validate the intensity rate in the image is offered in Eq. (2).

$$zu_{cg,dg} = \underset{(ad,bd)=\vartheta}{MED}\left(IM_{cg+ad,dg+bd}\right) \tag{2}$$

The windows presented in the image are offered, and the acquired median filtered images are defined and provided as the input to the feature extraction phase. The pre-processed outcome of dataset 1 and dataset 2 are provided in Figure 3.

Description	Sample Image 1	Sample Image 2	Sample Image 3	Sample Image 4	Sample Image 5
Dataset 1					
Dataset 2		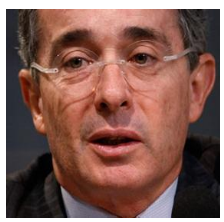			

Fig. 2 Sample face images from dataset 1 and dataset 2

4.2. Dual Feature Extraction Phase

In the dual feature extraction phase, the pre-processed images IM_q^a are utilized as input for LBP and 3-DWT to attain the spatial and spectral features accordingly.

LBP [31]: It utilized the pre-processed images IM_q^a as the input. LBP is a visual descriptor utilized to perform effective computer vision categorization. It is termed as highly powerful in classifying the texture features, and also they are fused with histogram-based descriptors to enhance the efficacy of detection. It effectively validates the binary pattern of every pixel in the image. Here, the essential binary patterns of the cell are attained by contrasting the intensity of the centre pixel in the neighbourhood of circular symmetrical. The counts of a neighbour pixel near the centre pixel are termed NC the radius of the symmetrical area, and the centre pixel value is offered as GC. The nearby pixels are termed as $GN = (N = 0, \ldots, NC - 1)$, where the pixel centre CP is weighted with the nearby pixel one by one, and the bitwise binary pattern associated with the centre pixel is created based on Eq. (3) and Eq. (4).

$$CP = [Sn(G_0 - GC), (G_1 - GC), \ldots, (G_{NC-1} - GC)] \tag{3}$$

$$S(N) = \begin{cases} 1, N \geq 0 \\ 0, N \leq 0 \end{cases} \tag{4}$$

The decimal number of the LBP is validated based on Eq. (5), along with corresponding weights.

$$LBP_{NC,SR} = \sum_{N=0}^{NC-1} S(G_N - GC)\, 2^N \tag{5}$$

Image Description	Image 1	Image 2	Image 3	Image 4	Image 5
Dataset 1					
Original Image					
Pre-Processed Image					
Dataset 2					
Original Image				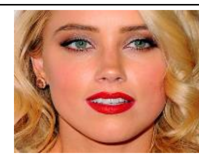	
Pre-Processed Image	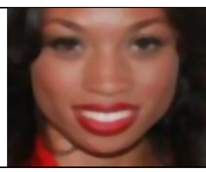				

Fig. 3 Pre-processed results of dataset 1 and dataset 2

At last, the histogram occurrences in various binary patterns are validated to generate a feature presentation of an image. The attained spatial features from LBP are termed FE_w^{lbp} and offered as the optimal feature selection phase input.

3-DWT [32]: It uses pre-processed images IM_q^a as the input. DWT is a transform approach commonly utilized in image processing, watermarking and compression. Here, the transformation is performed by a minute wave identified by the wavelet with modified frequency ranges and imperfect length. The wavelet rearranges the decomposed image into three different spatial instructions: diagonal, vertical, and horizontal.

Thus, the wavelet displays the histogram-based anisotropic nature with more accuracy. In this case, 3-DWT accuracy is maximal at Lower Band (LB) for every degree of decay, and it is minimal for other bands like HL, HH, and LH. Later, a 2-D modification is performed by utilizing the two separations in a 1-D transform.

Initially, images are separated with the unknown measurement with minimal skip and maximal skip procedure, where the filtered coefficients of minimal skip are placed in the matrix left part, and maximal bypass is filtered correctly. Decimation performed in the entire length of the transformed image remains identical. The 3-DWT is commonly applied in 3-D image compression. In 3-DWT, the low-pass filter outcome is again filtered to yield a better resolution rate. The acquired spectral features from 3-DWT are termed FE_e^{3dwt} and offered as the optimal feature selection phase input.

4.3. Implemented ACSP-WHO-Based Parameter Optimization

A novel ACSP-WHO is designed and implemented in the face recognition and verification framework for tuning the parameters like learning rate and hidden neuron count in DNN degree and maximum iteration in SVM and estimator count in Adaboost to provide better face recognition and classification rate.

WHO [29] is simple, easy to use, has better efficacy than the classical models, and offers better outcome rates by solving optimization problems. However, it has minimal exploration and searchability and quickly falls into local optima issues. Thus, to resolve the above-listed complications in the WHO, a novel ACSP-WHO technique is designed. The random number r presented in the range [0,1] is improvised by the newly designed concept offered in Eq. (6).

$$r = \frac{\left(2\sqrt{\frac{(PC*Maxiter)}{Npop}}\right)+PE}{I} \tag{6}$$

Here, the term PC indicates the crossover percentage, PEdenote the stallion percentage, Maxiter be the maximum iteration count, I be the iteration, and Npop be the number of population.

WHO: Generally, horses are classified into two classes non-territorial and territorial. Here, more contrasts are obtained between the two bonding categories: social character, mating, grazing, dominance, and leadership quality. Non-terrestrial horses are the horse group that has stable family groups with a stallion and mares. The significant phases of the wild horse optimizer are elaborated as follows.

Generate initial population: The initial random population of the algorithm is offered as $(\vec{a}) = \{\vec{a}_1, \vec{a}_2, \dots, \vec{a}_m\}$, and also, the target function utilized to validate the random population is termed as$(\vec{B}) = \{B_1, B_2, \dots, B_m\}$.

At first, the population is divided into different classes. If M is determined as the population member and the group count is termed as H = [M x PE], where PE representing the stallion percentage in the entire population, they are determined as the control parameter in the optimization model. Here, the leader based on the group count is offered as H(Stn) and also, the balance members presented in the group are separated equally in the group are given as(M-H). In the initial phases, the leaders of the groups are chosen randomly; further, they are selected according to fitness among the members present in the group.

Grazing Character: The foals spend more time grazing with their group. Here, the grazing character is implemented by considering the stallion at the centre of the grazing region with other members. The grazing character of the group members with more radiuses is equated in Eq. (7).

$$\bar{A}^d_{c,H} = 2E\,cos(2\pi FG) \times \left(Stn^d - A^d_{c,H}\right) + Stn^d \qquad (7)$$

The present position of the group member is termed as$A^d_{c,H}$, the stallion leader position is offered asStn^d, a uniform random number presented in the limit of $[-2,2]$ is given as F and pi is represented as π equal to the value 3.14. The novel position of group member at the time of grazing is termed as$\bar{A}^d_{c,H}$, and the adaptive mechanism is given as G , and it is equated in Eq. (8).

$$G = r \quad \Theta DX + \vec{r}_3 \Theta(\sim DX) \qquad (8)$$

Where $I = \vec{r}_1 < DR; DX = (I == 0)$in the above equation and the vector holds the values of 0 and 1 is termed as I. Random numbers with uniform distribution in the limit of [0,1] are given as, r and they are updated by the new concept offered in Eq. (6) and the random vectors in the range of $[0,1]$ is offered as $\vec{r}_1$ and $\vec{r}_3$ in the adaptive mechanism.

The term DX denotes the satisfying condition and adaptive parameter offered DR, which starts from the value one and is reduced when validation is performed in the approach based on Eq. (9). At the final stage of the validation, the algorithm reaches 0.

$$DR = 1 - itr \times \left(\frac{1}{Maxitr}\right) \qquad (9)$$

Here, the term Matrix indicates the maximal count of iteration, and the term itr is the present iteration.

Mating Character : Here, the foals are separated from their group and join other groups to reach puberty and search for a better match and mate. The character of leaving and mating of the horse is explained in Eq. (10) with a crossover operator X.

$$A^w_{H,J} = X\left(A^x_{H,c}, A^y_{H,d}\right) \qquad (10)$$

Where $c \neq d \neq J, w = x == endandX = mean$ are the terms presented in the above equation. Here, the horse $w$from the group $I$is given as$A^w_{H,J}$. The foal position x from the group$c$in the departure group is given as$A^x_{H,c}$, and also, after reaching the puberty age and mated by the horse $y$with the relived group, is termed as$A^y_{H,d}$.

Group leadership: The group leader should be able to lead the group members in a suitable environment, like a water hole. One group leader leads the members to the water hole, and other groups of foals move forward to the water hole.

Here, both leaders compete for the waterhole, so the team with high domination utilizes it, and other group members are not allowed to utilize it until they move away. In Eq. (11), the dominating characteristics are elaborated.

$$\overline{Stn_{H_c}} = \begin{cases} 2E\,cos(2\pi FG) \times \left(HW - Stn_{H_c}\right) + HW & if r_3 > 0.5 \\ 2E\,cos(2\pi FG) \times \left(HW - Stn_{H_c}\right) - HW & if r_3 \leq 0.5 \end{cases} \qquad (11)$$

Here, the leader's next position is termed $\overline{Stn_{H_c}}$for the group c, and the position of water hole is offered HW.

Leader Selection: In this approach, leaders are selected randomly, but later, leaders are chosen based on a fitness function. If a group member's fitness is better than the leader, then the leader's and member's positions are modified based on Eq. (12).

$$Stn_{H_c} = \begin{Bmatrix} A_{H,c} \ if \ cos \, y\left(A_{H,c}\right) < cos \, y\left(Stn_{H_c}\right) \\ Stn_{H_c} \, f \ cos \, y\left(A_{H,c}\right) < cos \, y\left(Stn_{H_c}\right) \end{Bmatrix} \quad (12)$$

The present leader position in the group$c$is given asStn_{H_c}in the above equation. The pseudocode of the recommended ACSP-WHO is offered in Algorithm 1. The flowchart for the recommenced ACSP-WHO is offered in Figure 4.

Algorithm 1: Developed ACSP-WHO
Initiate the population of horses randomly.
Initialize the parameters of $PC = 0.13$and $PE = 0.2$
Validate the horse's fitness.
Generate foals group and choose stallions.
Select the good horse as optimum.
Update$r$by new concept offered in Eq. (6)
While (Fulfilling end condition)
Validate $DR$by Eq. (8)
For stallions count
Validate Gusing Eq. (7)
For foals in any group
If $rand > PC$
Upgrade the foal position by Eq. (9)
Else
Upgrade the foal position by Eq. (10)
End If
End For
If $rand > 0.5$
Renew the position of the stallion by Eq. (11)
Else
Renew the position of the stallion by Eq. (12)
End If
End While
Renew the optimal solution.

4.4. Optimal Feature Selection with Developed ACSP-WHO

In this phase, the optimal features are attained by utilizing the developed ACSP-WHO. Here, the LBP-based spatial features$FE_w^{lbp}$and the 3-DWT-based spectral features$FE_e^{3dwt}$are concatenated to attain an effective face recognition and verification rate. Then the concatenated features are termed $FE_d^{CF} = \left(FE_e^{lbp}, FE_e^{3dwt}\right)$and utilized as the input for optimal feature selection. Here, the optimal features are attained from the concatenated features $FE_d^{CF}$and obtained in the range of [1,10] the developed ACSP-WHO. The attained optimal features are termed $FE_v^{opt}$and used as the input in ELNet for face recognition and classification. The structural view of recommended ACSP-WHO-based optimal feature selection is offered in Fig. 5.

5. Architectural Description of Ensemble Deep Learning-Based Efficient Face Recognition and Verification Framework

5.1. SVM

The inspiration of the structural risk minimization model initiates SVM [33, 34]. The SVM decision function for binary classification is offered in Eq. (13).

$$y(l) = \left(q, \varphi(l)\right) + d \quad (13)$$

Mapping for the sample$l$is termed as $\varphi(l)$from the input region to the superior dimensional feature space, and the optimal values are termed as$q$and$d$, which is utilized to resolve the optimization issue.

$$h(q, \xi) = \frac{1}{2}\|q\|^2 + J\sum_{z=1}^{M} \xi_z \quad (14)$$

$$x_z\left(\left(q, \varphi(l_z)\right) + i\right) \geq 1 - \xi_z; \rightleftarrows \xi_z \geq 0 \quad (15)$$

The slack variable is termed as ξ_z, and the regularisation parameter is referred to as ξ_z . The minimization issues are offered in Eq. (16).

$$V(\alpha) = -\sum_{z=1}^{M} \alpha_z + \frac{1}{2}\sum_{z=1}^{M}\sum_{p=1}^{M} x_z x_p \, \alpha_z \alpha_p O\left(l_z, l_p\right) \quad (16)$$

$$\sum_{z=1}^{M} x_z \, \alpha_z = 0; \forall z: 0 \leq \alpha_z \leq J \quad (17)$$

Here, the Lagrange multiplier is termed as that related to the sample $l_z$in the above equation. The kernel function represents the maps in the input vector with the appropriate feature space referred to$O(\quad)$, and it is offered in Eq. (18).

$$O\left(l_z, l_p\right) = \left(\varphi(l_z), \varphi\left(l_p\right)\right) \quad (18)$$

Using the kernel function, SVM can automatically validate the weights, thresholds and centres.

5.2. DNN

DNN [35] structure utilizes three essential elements: hidden layer, output layer and input layer. They are developed with two hidden neurons to learn the essential mapping correlation over the output and input data, which are considered the initial fitness weight. The node weights presented in the hidden layer are improvised on the training region.

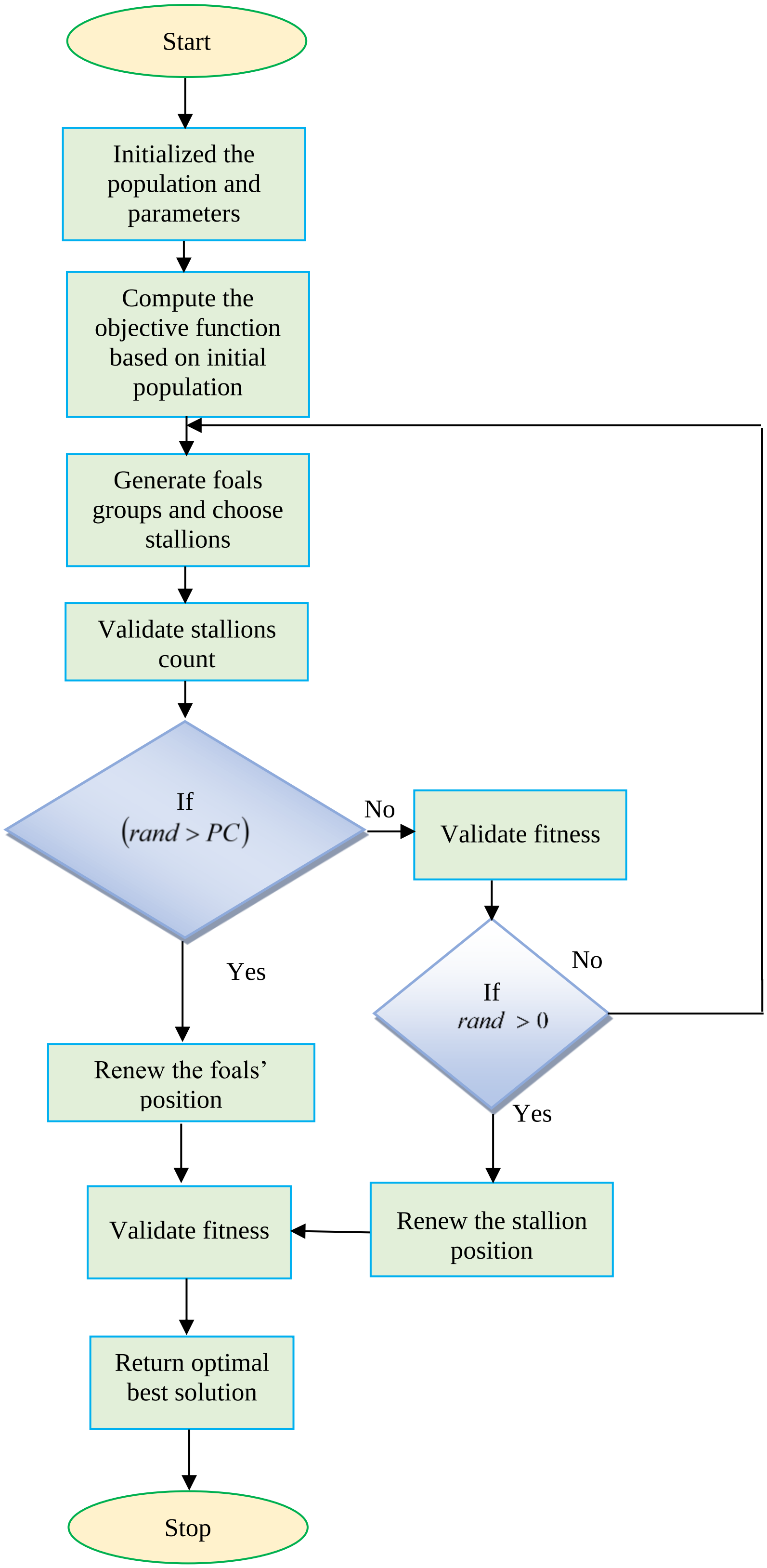

Fig. 4 Flowchart of developed ACSP-WHO

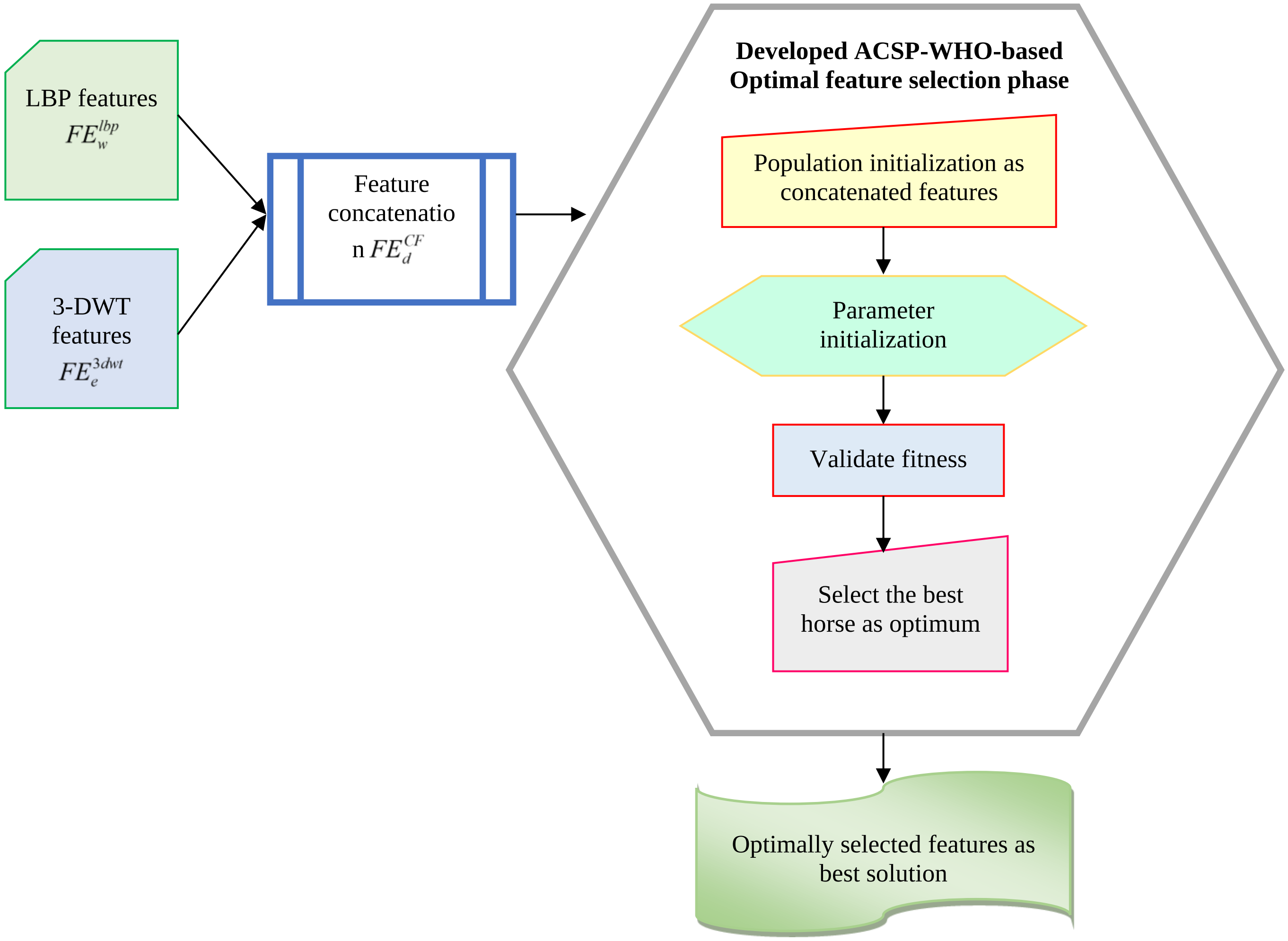

Fig. 5 Diagrammatic view of developed ACSP-WHO-based optimal feature selection

Here, training iterations are improved due to the presence of a neural network, and their frequencies are fitted frequently in the region of labelled training data.

Moreover, hidden neurons are implemented to enhance the verification accuracy rate and speed up the training process in DNN. The entire number of nodes presented in the hidden layers is validated by Eq. (19).

$$T = \sqrt{yi + ui + pi} \tag{19}$$

The constant value ranges from the limit [1,10] as pi nodes count in the output layer is offered ui, node count in the input layer is offered yi, and the count of nodes in the hidden neuron is termed as T.

The activation function holds the hidden layer for permitting the fitness of a non-linear function. The activation function is termed sigmoid and is offered in Eq. (20).

$$Z = \frac{1}{1+e^{-FE_v^{opt}}} \tag{20}$$

Here, the optimal features FE_v^{opt} are offered as the input, and the function of mapping Rp with the activation network in the input data is presented in Eq. (21).

$$R_p = sigmoid(\rho_l E + \alpha_l) \tag{21}$$

The biases in the hidden layer are termed as α, and also, the weights of the matrix in the output layer are termed as ρ in the equation.

5.3. Adaboost

Adaboost [36] is utilized to classify the critical optimal features without overfitting issues. Initially, Adaboost is distributed uniformly. Then, it utilized the component learning approach in the sequence cycle. In the initial cycle A, Adaboost offers the training samples U_l for the component learn distribution. In this phase, the com ponent teaches effectively trains the classifier H_l and also the distribution U_l is renewed in every cycle based on the verification outcome in the training samples.

Here, the easy samples are categorized accurately, where H_l attain the minimal weights, and also, the complex samples are misclassified and secured the maximal weights. So, the Adaboost always concentrate the samples with maximal weights, which is more complex for learning. The learning process exists up to B cycles. At last, Adaboost fuses entire component classifiers as a single hypothesis in a linear format. Then, the maximal weights are offered to the component classifier with minimal training errors.

5.4. Developed ELNet-based Face Recognition and Verification Method

The main objective in designing ELNet is to offer better face recognition and verification rate. SVM has superior dimensional space with more efficacy rate and also has more storage space. However, they do not apply to large datasets and face overlapping issues when the data is offered with more noise.

DNN effectively learn complex features and efficiently performs complicated validation task. Still, it needs enormous data, and its validation is more expansive. Later, Adaboost is utilized as it has minimal overfitting issues, but it uses only a superior and high-quality dataset for the analysis.

Thus, a new ensemble approach, ELNetis, was developed to attain effectual face recognition and prediction rate. Finally, face recognition and verification outcome is attained as the classified face reactions from the images by verifying the faces and recognizing them through the developed ELNet model by averaging SVM, DNN and Adaboost scores.

The parameters in SVM, like degree, are tuned in the range of [1,5] and also, the maximal iteration count is optimized in the range of $[50{,}100]$, DNN learning rate is tuned in the limit of $[0.01{,}0.99]$ and the hidden neurons are tuned in the limit of $[5{,}255]$.

Finally, the estimator count in Adaboost is tuned in the limit of $[1{,}100]$ by the developed ACSP-WHO to maximize accuracy. The fitness function of the developed ELNet-based face recognition and verification framework is offered in Eq. (22).

$$FT = \underset{\{DE_b^{svm}, MI_l^{svm}, HN_q^{dnn}, LR_i^{dnn}, ES_g^{ada}\}}{argmax} (ACUY) \quad (22)$$

Here, the SVM degree is indicated as DE_b^{svm}, maximum iteration in SVM is termed as MI_l^{svm}, hidden neuron count in DNN is referred to as HN_q^{dnn} learning rate in DNN is presented as LR_i^{dnn} and the estimators of Adaboost are represented as ES_g^{ada} in the above fitness equation. The term $ACUY$ indicates accuracy, the validation of closeness in a specific value, and is offered in Eq. (23).

$$ACUY = \frac{(Yi+Yj)}{(Yi+Yj+Ys+Yt)} \quad (23)$$

The false negative value is offered as Yt the true positive is given as Yi the false positive is termed as Ys, and the true negative is presented as Yj. The pictorial presentation of the ELNet-based face recognition and verification framework is offered in Figure 6.

6. Results and Discussion

6.1. Experimental Setup

A new face recognition and verification framework was developed and implemented in Python. Further, different analyses were executed in the recommended framework with multiple verification models and algorithms. In the developed face recognition and verification framework, a better efficacy rate was attained by utilizing the population count as 10, maximum iteration count as 25 and chromosome length as 15. Various approaches contrasted over the developed model were Deer Hunting Optimization Algorithm (DHOA) [38], Barnacles Mating Optimizer (BMO) [40], African Vultures Optimization Algorithm (AVOA) [38], and WHO [29] and different verification models like CNN [40], SVM [33], DNN [35], Adaboost [36] and SVM-DNN-ADB [32, 31].

6.2. Performance Metrics

The standard measures employed to validate the efficacy of the developed model are elaborated as follows.

(a) False Discovery Rate (FDR) is formulated in Eq. (24).

$$FDR = \frac{Ys}{Ys+Yi} \quad (24)$$

(b) Precision is indicated as pc and formulated in Eq. (25).

$$pc = \frac{Yi}{Yi+Ys} \quad (25)$$

(c) FalseNegative Rate (FNR)is shown in Eq. (26).

$$FNR = \frac{Yt}{Yi+Yj} \quad (26)$$

(d) F1 score is offered in Eq. (27).

$$F1 - score = \frac{2Yi}{2Yi+Ys+Tt} \quad (27)$$

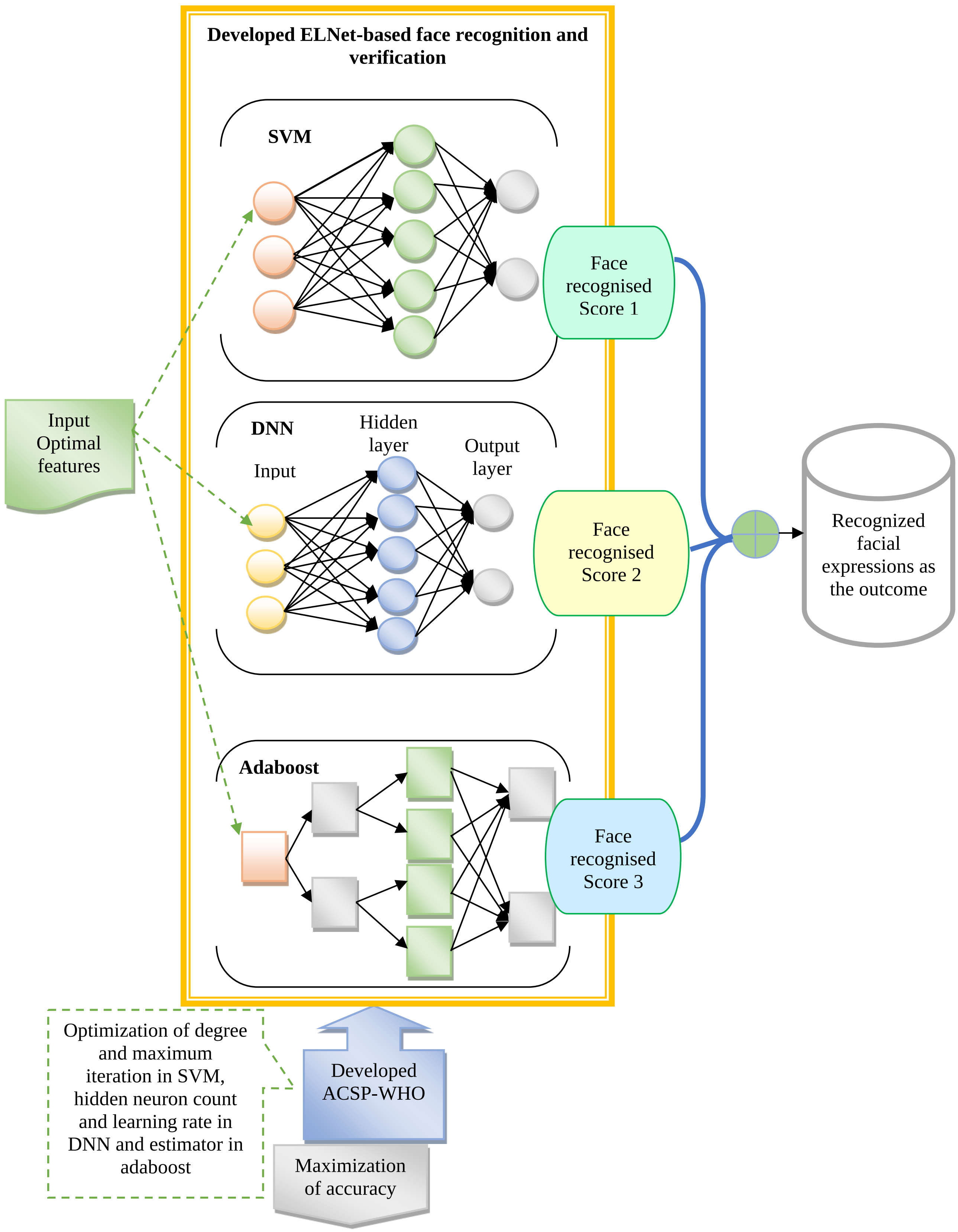

Fig. 6 Architectural view of ELNet-based face recognition and verification model

(e) Negative Predictive Value (NPV) is derived in Eq. (28).

$$NPV = \frac{Yj}{Yt+Yj} \tag{28}$$

(f) Sensitivity is derived in Eq. (29).

$$Se = \frac{Yi}{Yi+Yt} \tag{29}$$

(g) Mathews Correlation Coefficient (MCC) is equated in Eq. (30).

$$MCC = \frac{Yi\times Yj - Ys\times Yj}{\sqrt{(Yi+Ys)(Yi+Yt)(Yj+Ys)(Yj+Yt)}} \tag{30}$$

(h) Specificity is formulated in Eq. (31).

$$Spc = \frac{Yj}{Yj+Ys} \tag{31}$$

(i) False positive rate (FPR)is given in Eq. (32).

$$FPR = \frac{Ys}{Ys+Yj} \tag{32}$$

6.3. Dataset 1-Related Validation on Developed Face Verification Model

Multiple analyses performed in the suggested model over different face verification models and algorithms in dataset 1 are given in Fig. 7 and Fig. 8.

Table 2. Validation of developed face recognition and verification model with classical algorithms in dataset 1 and dataset 2

Metrics	DHOA-ELNet [38]	AVOA-ELNet [39]	BMO-ELNet [40]	WHO-ELNet [29]	ACSP-WHO-ELNet
Dataset 1					
Accuracy	92.32206	93.55634	94.62534	94.97011	96.44557
Sensitivity	92.24286	93.54286	94.65714	95.01429	96.45714
Specificity	92.32222	93.55637	94.62528	94.97003	96.44555
Precision	2.351061	2.826995	3.40905	3.647421	5.157781
FPR	7.677784	6.44363	5.374721	5.029974	3.554452
FNR	7.757143	6.457143	5.342857	4.985714	3.542857
NPV	92.32222	93.55637	94.62528	94.97003	96.44555
FDR	97.64894	97.173	96.59095	96.35258	94.84222
F1-Score	4.585254	5.488132	6.581084	7.02516	9.791964
MCC	0.140497	0.156533	0.174172	0.180904	0.218744
Dataset 2					
Accuracy	92.31733	93.56	94.60533	94.94933	96.464
Sensitivity	92.13333	93.46667	94.53333	94.8	96.4
Specificity	92.32109	93.5619	94.6068	94.95238	96.46531
Precision	19.6698	22.85621	26.34708	27.7085	35.75668
FPR	7.678912	6.438095	5.393197	5.047619	3.534694
FNR	7.866667	6.533333	5.466667	5.2	3.6
NPV	92.32109	93.5619	94.6068	94.95238	96.46531
FDR	80.3302	77.14379	73.65292	72.2915	64.24332
F1-Score	32.41848	36.73042	41.20895	42.88299	52.1645
MCC	0.405776	0.444608	0.483537	0.497683	0.575629

The developed ACSP-WHO-ELNet-based face recognition and verification model secured 14.6% better than CNN, 13.2% enhanced than SVM, 10.5% improved than DNN, 8.04% superior to ADABOOST and 4.44% greater than SVM_DNN_ADB in accuracy analysis.

6.4. Dataset 2-Based Validation on Initiated Face Verification Model

Different analyses performed in the recommended face recognition and verification framework over multiple verification schemes and algorithms are displayed in Fig. 9 and Fig. 10. F1-Score analysis performed in the suggested face recognition and verification model is contracted over different existing approaches and attained better efficacy rates as 10.4%, 869%, 72%, 48.27% and 19.4% correspondingly for CNN, SVN, DNN, ADABOOST, and SVM_DNN_ADB.

6.5. Overall Validation of Suggested Face Recognition and Verification Framework

Analysis of the developed face recognition and verification framework over the different algorithms and existing verification models are displayed in Table 2 and Table 3. Accuracy analysis performed on the suggested face recognition and verification technique secured 4.46%, 3.08%, 1.92% and 1.55% better than the classical approaches like DHOA-ELNet, AVOA-ELNet, BMO-ELNet and WHO-ELNet, correspondingly in dataset 1.

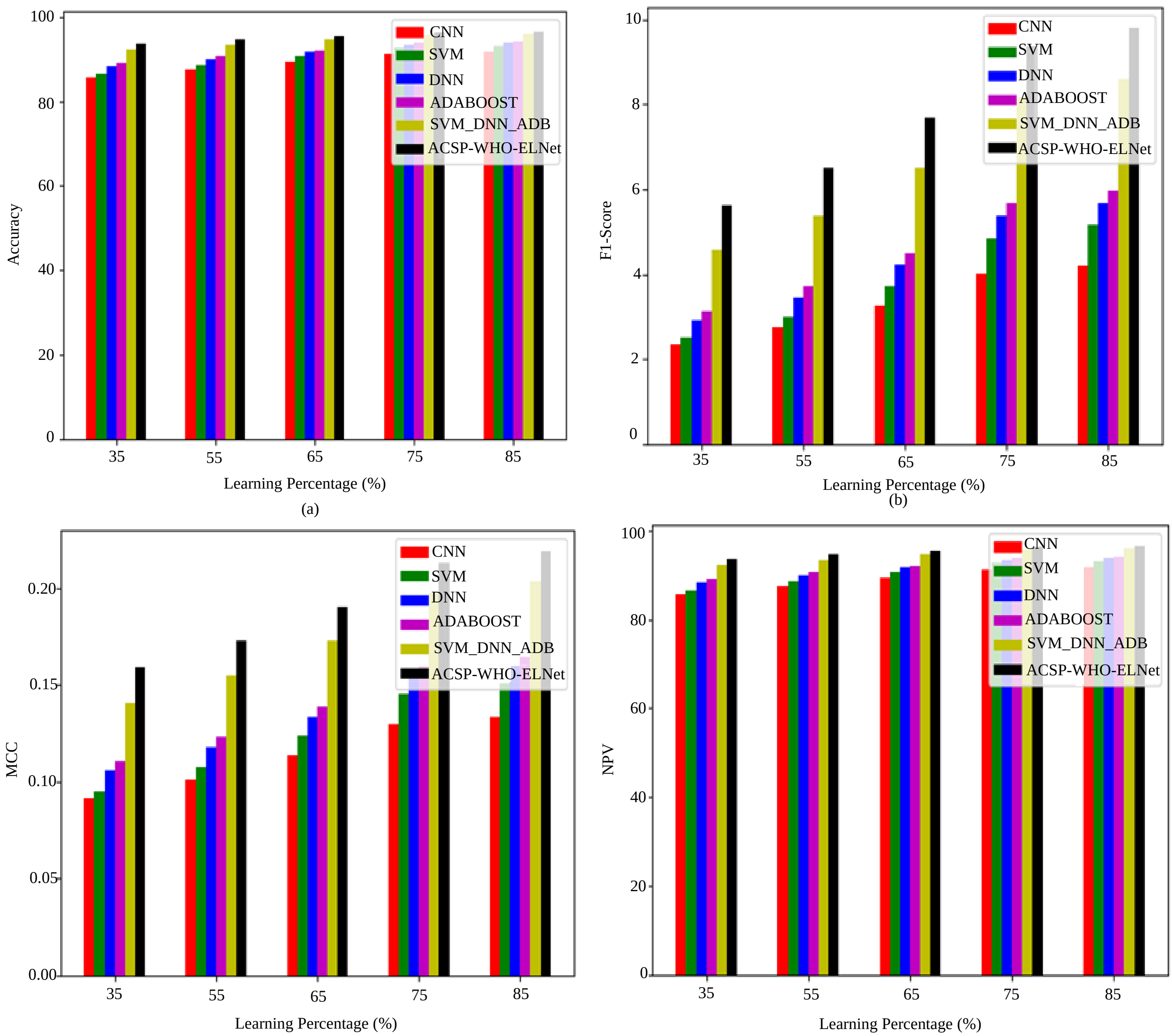

(a) (b) (c) (d)

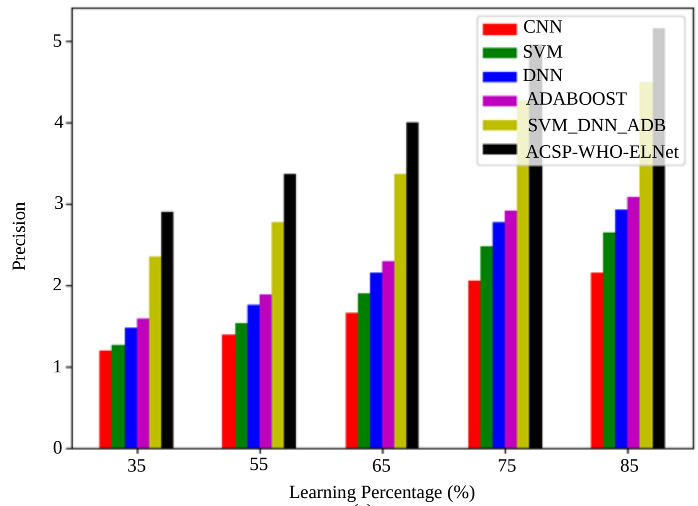

(e)

Fig. 7 Analysis of the recommended face recognition and verification model over existing verification models in dataset 1 with (a) Accuracy, (b) F1-Score, (c) MCC, (d) NPV and (e) Precision

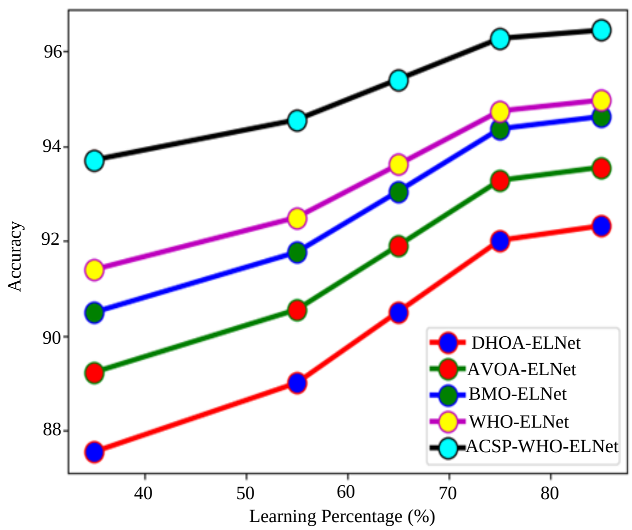

(a)

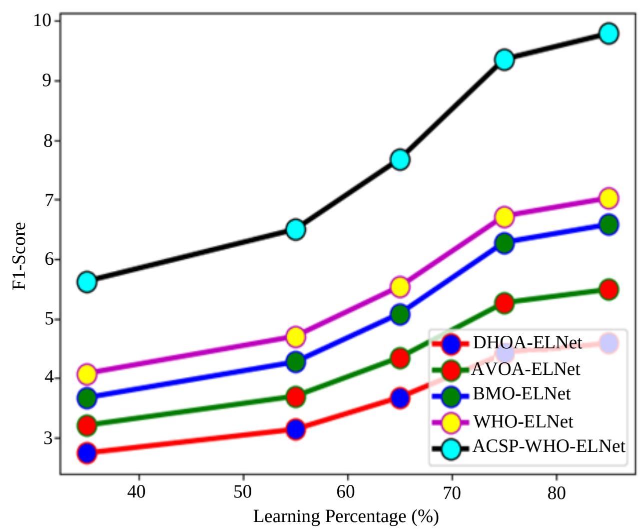

(b)

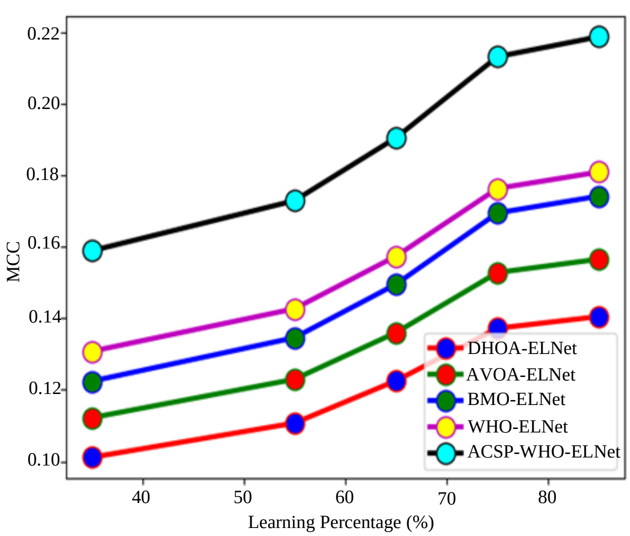

(c)

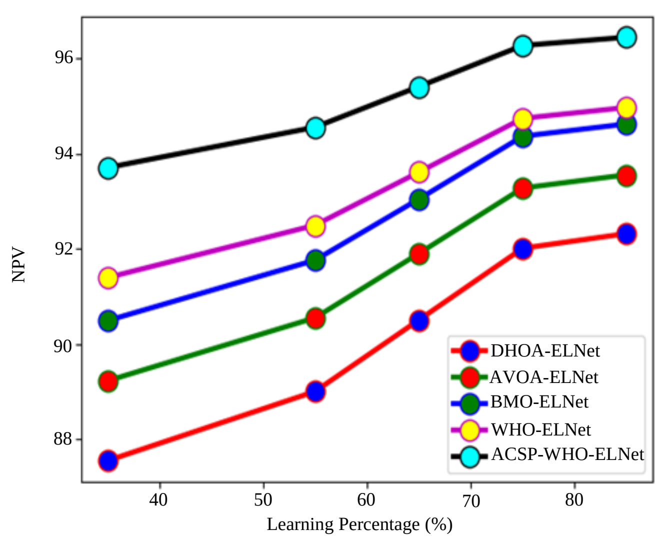

(d)

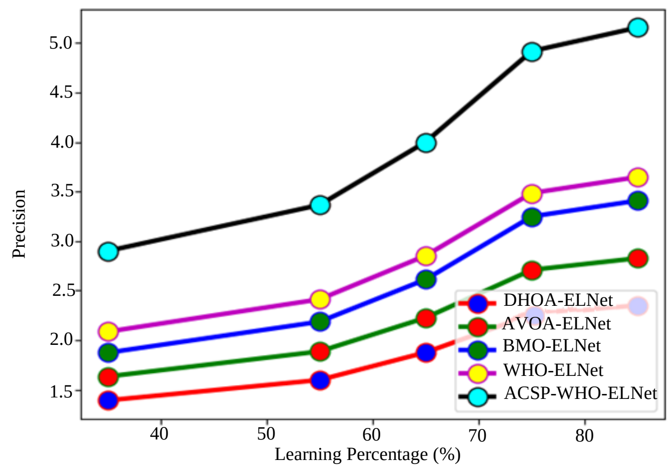

(e)

Fig. 8 Analysis of the recommended face recognition and verification model over existing algorithms in dataset 1 with (a) Accuracy, (b) F1-Score, (c) MCC, (d) NPV and (e) Precision

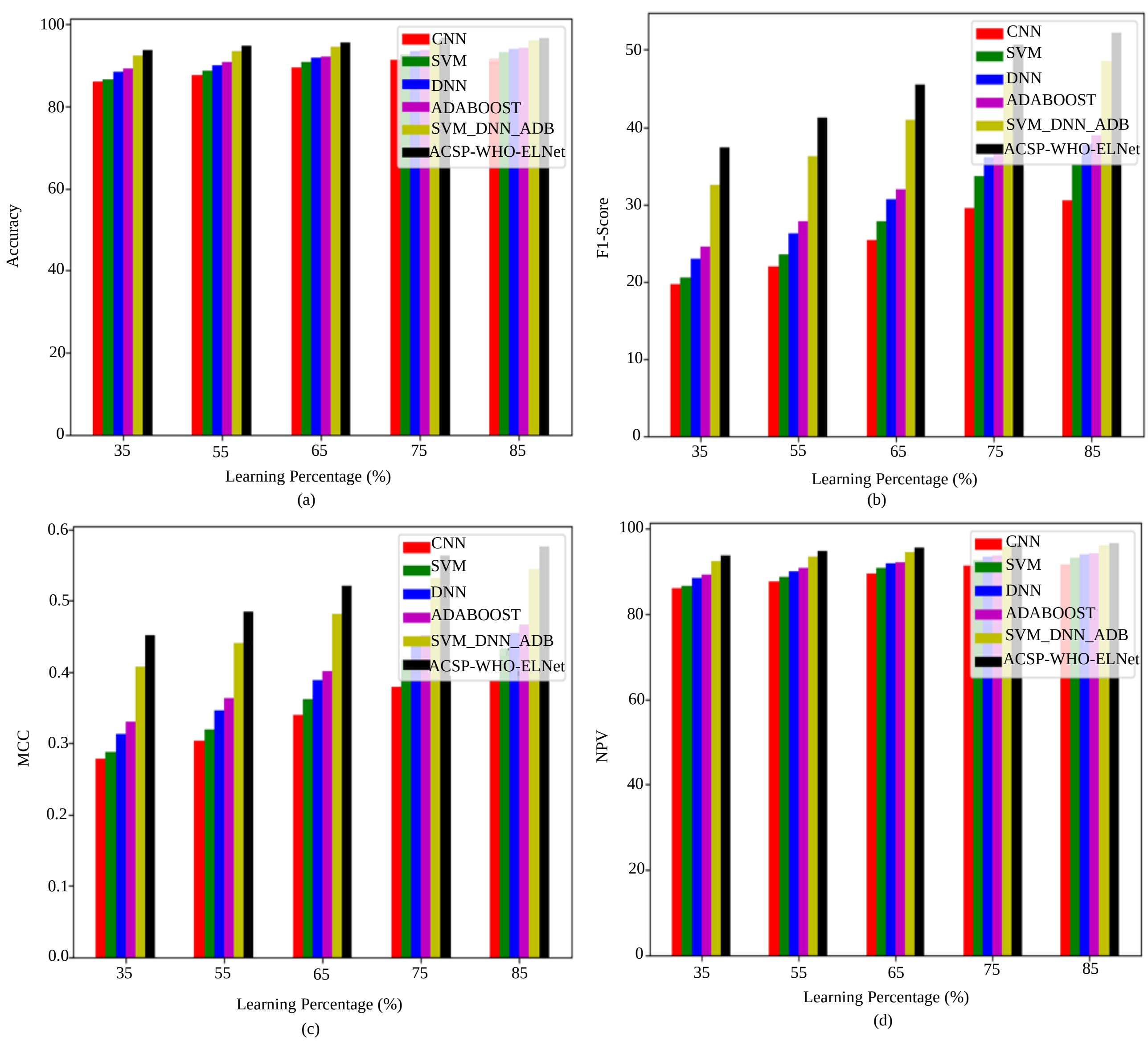

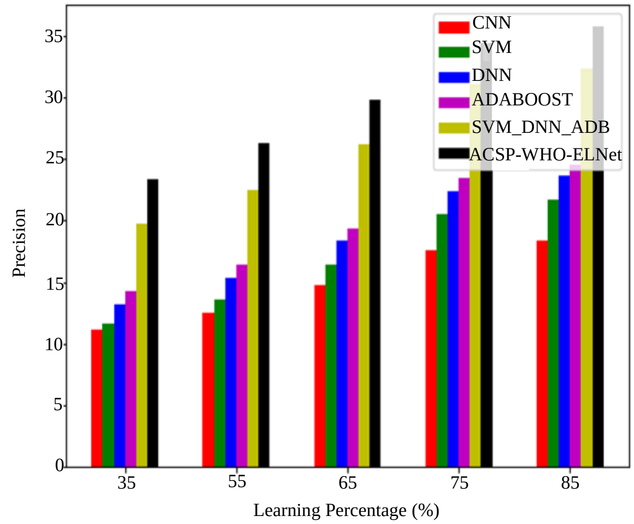

(e)

Fig. 9 Analysis of suggested face recognition and verification model over existing verification models in dataset 2 with (a) Accuracy, (b) F1-Score, (c) MCC, (d) NPV and (e) Precision

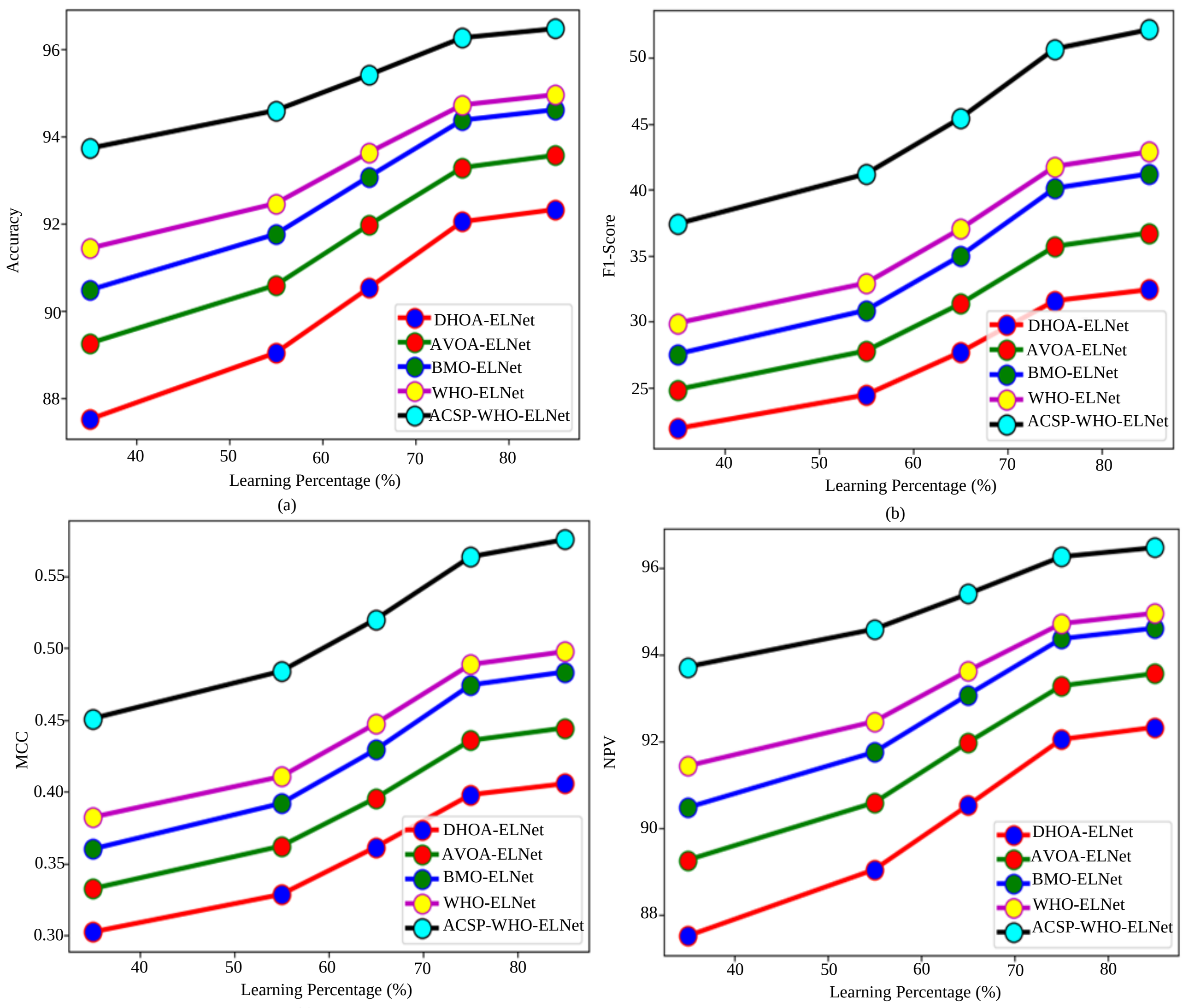

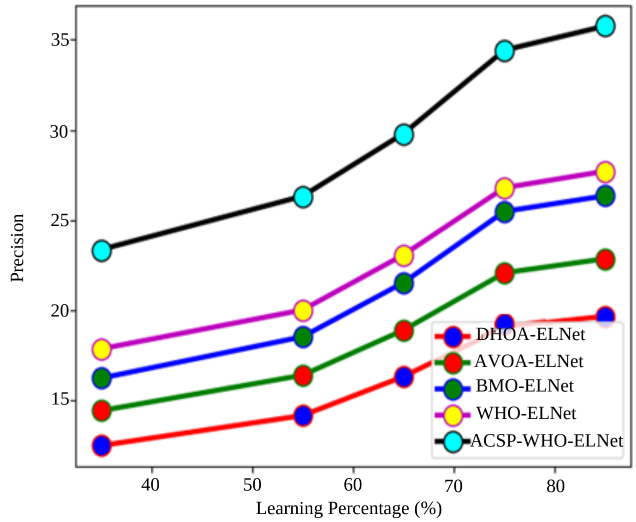

(e)

Fig. 10 Analysis of the suggested face recognition and verification model over existing algorithms in dataset 2 with (a) Accuracy, (b) F1-Score, (c) MCC, (d) NPV and (e) Precision

Table 3. Validation of suggested face recognition and verification model with different verification techniques in dataset 1 and dataset 2

Metrics	CNN [37]	SVM [33]	DNN [35]	ADABOOST [36]	SVM_DNN_ADB [32, 31]	ACSP-WHO-ELNet
Dataset 1						
Accuracy	91.66131	93.14474	93.78123	94.084	95.926	96.44557
Sensitivity	91.57143	93.14286	93.65714	94.04286	95.9	96.45714
Specificity	91.66149	93.14475	93.78148	94.08408	95.92605	96.44555
Precision	2.153362	2.650687	2.929807	3.087335	4.504885	5.157781
FPR	8.338506	6.855253	6.218523	5.915918	4.073948	3.554452
FNR	8.428571	6.857143	6.342857	5.957143	4.1	3.542857
NPV	91.66149	93.14475	93.78148	94.08408	95.92605	96.44555
FDR	97.84664	97.34931	97.07019	96.91267	95.49511	94.84222
F1-Score	4.207776	5.15468	5.681872	5.978404	8.605528	9.791964
MCC	0.133303	0.150814	0.159685	0.164608	0.203194	0.218744
Dataset 2						
Accuracy	91.656	93.13333	93.82133	94.09333	95.91467	96.464
Sensitivity	91.86667	93.2	94	94.13333	96	96.4
Specificity	91.6517	93.13197	93.81769	94.09252	95.91293	96.46531
Precision	18.3391	21.68787	23.68156	24.53945	32.40324	35.75668
FPR	8.348299	6.868027	6.182313	5.907483	4.087075	3.534694
FNR	8.133333	6.8	6	5.866667	4	3.6
NPV	91.6517	93.13197	93.81769	94.09252	95.91293	96.46531
FDR	81.6609	78.31213	76.31844	75.46055	67.59676	64.24332
F1-Score	30.57466	35.18752	37.83204	38.93025	48.45222	52.1645
MCC	0.38943	0.431221	0.454776	0.464091	0.545019	0.575629

6.6. Statistical Analysis of the Developed Model

Statistical observation performed on the suggested face recognition and verification framework over dataset 1 and dataset 2 is displayed in Table 4.

The best analysis performed on the recommended face recognition and verification model secured 1.91% better than DHOA-ELNet, 0.58% improved than AVOA-ELNet, 8.86% superior to BMO-ELNet, and 1.21% higher thanWHO-ELNet in dataset 2.

6.7. Computation Time Analysis on the Developed Model

Computational time analysis performed on the suggested face recognition and verification model in dataset 1 and dataset 2 are tabulated in Table 5 and Table 6.

Time consumption analysis performed on the ACSP-WHO-ELNet-based face recognition and verification model in dataset 1 secured 8.9%, 12.5%, 4.3% and 5.4% higher than DHOA-ELNet, AVOA-ELNet, BMO-ELNet and WHO-ELNet, correspondingly.

Table 4. Statistical analysis of the developed face recognition and verification model over different algorithms

Metrics	DHOA-ELNet [38]	AVOA-ELNet [39]	BMO-ELNet [40]	WHO-ELNet [29]	ACSP-WHO-ELNet
Dataset 1					
Best	1.004365	1.004811	1.00608	1.004358	1.003891
Worst	1.182844	1.029913	1.026872	1.113382	1.034115
Mean	1.017992	1.026435	1.011055	1.012599	1.011568
Median	1.013335	1.028924	1.00608	1.006361	1.004724
Standard Deviation	0.034013	0.006565	0.008854	0.023053	0.009439
Dataset 2					
Best	1.00312	1.001792	1.010154	1.002419	1.001204
Worst	1.052227	1.047658	1.093006	1.043569	1.026117
Mean	1.012732	1.013571	1.018296	1.008499	1.008773
Median	1.00312	1.003545	1.010154	1.002419	1.001204
Standard Deviation	0.019168	0.01917	0.022616	0.012779	0.009733

Table 5. Computational time analysis on the suggested face recognition and verification model over algorithms

Metrics	DHOA-ELNet [38]	AVOA-ELNet [39]	BMO-ELNet [40]	WHO-ELNet [29]	ACSP-WHO-ELNet
Dataset 1					
Time (sec)	52.4577	59.4466	54.3788	55.2556	51.9887
Dataset 2					
Time (Sec)	35.3456	38.5782	36.5774	37.7557	33.8585

Table 6. Computational time analysis on the developed face recognition and verification framework over classical face verification models

Metrics	CNN [37]	SVM [33]	DNN [35]	ADABOOST [36]	SVM_DNN_ADB [32, 31]	ACSP-WHO-ELNet
Dataset 1						
Time (sec)	71.5744	74.79	76.5758	68.3468	65.3789	63.5688
Dataset 2						
Time (sec)	57.9077	62.3577	54.3467	53.7998	51.4367	48.5478

7. Conclusion

A new face recognition and verification framework was developed based on deep learning models to offer effectual recognition and verification rates in real-world scenarios. Essential data for the analysis were collected from the benchmark dataset and offered to pre-processing phase. Here, median filtering schemes were utilized to pre-process the image and subjected it to the feature extraction phase.

Here, two sets of LBP-based spatial features and 3-DWT-based spectral features were attained, concatenated, and forwarded to the optimal feature selection phase. In this phase, optimal features were attained by the developed ACSP-WHO and fed as the input to ELNet for practical face recognition and verification rate by maximizing the accuracy. Accuracy analysis performed on the suggested face recognition and verification technique secured 4.46%, 3.08%, 1.92% and 1.55% better than the classical approaches like DHOA-ELNet, AVOA-ELNet, BMO-ELNet and WHO-ELNet, correspondingly.

Hence, the initiated face recognition and verification framework secured a better face verification rate than the traditional approaches.

References

[1] Jiankang Deng, "ArcFace: Additive Angular Margin Loss for Deep Face Recognition," *2019 IEEE/CVF Conference on Computer Vision and Pattern Recognition (CVPR)*, Long Beach, CA, USA, pp. 4685-4694, 2019. [CrossRef] [Google Scholar] [Publisher Link]

[2] Stefanos Zafeiriou et al., "Regularized Kernel Discriminant Analysis with a Robust Kernel for Face Recognition and Verification," *IEEE Transactions on Neural Networks and Learning Systems*, vol. 23, no. 3, pp. 526-534, 2012. [CrossRef] [Google Scholar] [Publisher Link]

[3] Poornima Krishnan, and S. Naveen, "RGB-D Face Recognition System Verification using Kinect and FRAV3D Databases," *Procedia Computer Science*, vol. 46, pp. 1653-1660, 2015. [CrossRef] [Google Scholar] [Publisher Link]

[4] Baraa Adil Mahmood, and Sefer Kurnaz, "An Investigational FW-MPM-LSTM Approach for Face Recognition using Defective Data," *Image and Vision Computing*, vol. 132, p. 104644, 2023. [CrossRef] [Google Scholar] [Publisher Link]

[5] Prasanna Rajendra et al., "Smart Surveillance using OpenCV, Motion Analysis and Facial Landmark," *SSRG International Journal of VLSI & Signal Processing*, vol. 7, no. 1, pp. 11-14, 2020. [CrossRef] [Publisher Link]

[6] N. Asha et al., "Principal Component Analysis on Face Recognition using Artificial Fire Firefly Swarm Optimization Algorithm," *Advances in Engineering Software*, vol. 174, p. 103296, 2022. [CrossRef] [Google Scholar] [Publisher Link]

[7] Tongguang Ni et al., "Multi-Task Deep Metric Learning with Boundary Discriminative Information for Cross-Age Face Verification," *Journal of Grid Computing*, vol. 18, pp. 197-210, 2020. [CrossRef] [Google Scholar] [Publisher Link]

[8] Bilel Ameur et al., "Hybrid Descriptors and Weighted PCA-EFMNet for Face Verification in the Wild," *International Journal of Multimedia Information Retrieval*, vol. 8, pp. 143-154, 2019. [CrossRef] [Google Scholar] [Publisher Link]

[9] Ming Liu et al., "PA-GAN: A Patch-Attention Based Aggregation Network for Face Recognition in Surveillance," *IEEE Access*, vol. 8, pp. 152780-152789, 2020. [CrossRef] [Google Scholar] [Publisher Link]

[10] Dong Li, Huiling Zhou, and Kin-Man Lam, "High-Resolution Face Verification using Pore-Scale Facial Features," *IEEE Transactions on Image Processing*, vol. 24, no. 8, pp. 2317-2327, 2015. [CrossRef] [Google Scholar] [Publisher Link]

[11] Wonjun Hwang et al., "Face Recognition System using Multiple Face Model of Hybrid Fourier Feature under Uncontrolled Illumination Variation," *IEEE Transactions on Image Processing*, vol. 20, no. 4, pp. 1152-1165, 2011. [CrossRef] [Google Scholar] [Publisher Link]

[12] Shu Zhang et al., "DeMeshNet: Blind Face Inpainting for Deep MeshFace Verification," *IEEE Transactions on Information Forensics and Security*, vol. 13, no. 3, pp. 637-647, 2018. [CrossRef] [Google Scholar] [Publisher Link]

[13] Lingshuang Du, and Haifeng Hu, "Cross-Age Identity Difference Analysis Model Based on Image Pairs for Age Invariant Face Verification," *IEEE Transactions on Circuits and Systems for Video Technology*, vol. 31, no. 7, pp. 2675-2685, 2021. [CrossRef] [Google Scholar] [Publisher Link]

[14] Jinjin Liu et al., "CP-GAN: A Cross-Pose Profile Face Frontalization Boosting Pose-Invariant Face Recognition," *IEEE Access*, vol. 8, pp. 198659-198667, 2020. [CrossRef] [Google Scholar] [Publisher Link]

[15] Richard Jiang et al., "Face Recognition in the Scrambled Domain via Salience-Aware Ensembles of Many Kernels," *IEEE Transactions on Information Forensics and Security*, vol. 11, no. 8, pp. 1807-1817, 2016. [CrossRef] [Google Scholar] [Publisher Link]

[16] Xing Di et al., "Multi-Scale Thermal to Visible Face Verification via Attribute Guided Synthesis," *IEEE Transactions on Biometrics, Behavior, and Identity Science*, vol. 3, no. 2, pp. 266-280, 2021. [CrossRef] [Google Scholar] [Publisher Link]

[17] S. Zafeiriou et al., "Exploiting Discriminant Information in Nonnegative Matrix Factorization with Application to Frontal Face Verification," *IEEE Transactions on Neural Networks*, vol. 17, no. 3, pp. 683-695, 2006. [CrossRef] [Google Scholar] [Publisher Link]

[18] Bor-Chun Chen, Chu-Song Chen, and Winston H. Hsu, "Face Recognition and Retrieval using Cross-Age Reference Coding with Cross-Age Celebrity Dataset," *IEEE Transactions on Multimedia*, vol. 17, no. 6, pp. 804-815, 2015. [CrossRef] [Google Scholar] [Publisher Link]

[19] Ankit Jain et al., "An Overview on Facial Expression Perception Mechanisms," *SSRG International Journal of Computer Science and Engineering*, vol. 6, no. 4, pp. 19-24, 2019. [CrossRef] [Google Scholar] [Publisher Link]

[20] Heri Purwanto et al., "Design and Development of Mask Detectors in Effort to Prevent the Spread of Hepatitis Post-Covid-19 Pandemic using Viola-Jones Algorithm," *SSRG International Journal of Electronics and Communication Engineering*, vol. 10, no. 5, pp. 160-169, 2023. [CrossRef] [Publisher Link]

[21] Xinxing Xu, Wen Li, and Dong Xu, "Distance Metric Learning using Privileged Information for Face Verification and Person Re-Identification," *IEEE Transactions on Neural Networks and Learning Systems*, vol. 26, no. 12, pp. 3150-3162, 2015. [CrossRef] [Google Scholar] [Publisher Link]

[22] Yukun Ma et al., "A Secure Face-Verification Scheme Based on Homomorphic Encryption and Deep Neural Networks," *IEEE Access*, vol. 5, pp. 16532-16538, 2017. [CrossRef] [Google Scholar] [Publisher Link]

[23] Chun Pong Lau, Carlos D Castillo, and Rama Chellappa, "ATFaceGAN: Single Face Semantic Aware Image Restoration and Recognition from Atmospheric Turbulence," *IEEE Transactions on Biometrics, Behavior, and Identity Science*, vol. 3, no. 2, pp. 240-251, 2021. [CrossRef] [Google Scholar] [Publisher Link]

[24] Marios Kyperountas, Anastasios Tefas, and Ioannis Pitas, "Weighted Piecewise LDA for Solving the Small Sample Size Problem in Face Verification," *IEEE Transactions on Neural Networks*, vol. 18, no. 2, pp. 506-519, 2007. [CrossRef] [Google Scholar] [Publisher Link]

[25] Shervin Rahimzadeh Arashloo, and Josef Kittler, "Energy Normalization for Pose-Invariant Face Recognition Based on MRF Model Image Matching," *IEEE Transactions on Pattern Analysis and Machine Intelligence*, vol. 33, no. 6, pp. 1274-1280, 2011. [CrossRef] [Google Scholar] [Publisher Link]

[26] Xiaofeng Liu et al., "Dependency-Aware Attention Control for Image Set-Based Face Recognition," *IEEE Transactions on Information Forensics and Security*, vol. 15, pp. 1501-1512, 2020. [CrossRef] [Google Scholar] [Publisher Link]

[27] Baochang Zhang et al., "Local Derivative Pattern versus Local Binary Pattern: Face Recognition with High-Order Local Pattern Descriptor," *IEEE Transactions on Image Processing*, vol. 19, no. 2, pp. 533-544, 2010. [CrossRef] [Google Scholar] [Publisher Link]

[28] Abirami, Kavinila K, and Kavitha T, "Role of Machine Learning in Object Detection: A Review," *International Journal of Engineering Trends and Technology*, vol. 67, no. 5, 192-194, 2019. [CrossRef] [Publisher Link]

[29] Iraj Naruei, and Farshid Keynia, "Wild Horse Optimizer: A New Meta-Heuristic Algorithm for Solving Engineering Optimization Problems," *Engineering with Computers*, vol. 38, pp. 3025-3056, 2022. [CrossRef] [Google Scholar] [Publisher Link]

[30] Reecha Sharma, and M. S. Patterh, "A New Pose Invariant Face Recognition System using PCA and ANFIS," *Optik*, vol. 126, no. 23, pp. 3483-3487, 2015. [CrossRef] [Google Scholar] [Publisher Link]

[31] Youqi Zhang, Zhiyi Tang, and Ruijing Yang, "Data Anomaly Detection for Structural Health Monitoring by Multi-View Representation Based on Local Binary Patterns," *Measurement*, vol. 202, p. 111804, 2022. [CrossRef] [Google Scholar] [Publisher Link]

[32] Pooja Sharma, and Ashutosh Sharma, "Robust Technique for Steganography on Red Component using 3- DWT-DCT Transform," *2018 2nd International Conference on Inventive Systems and Control (ICISC)*, Coimbatore, India, pp. 1049-1054, 2018. [CrossRef] [Google Scholar] [Publisher Link]

[33] Vahid Azimirad, Mahdiyeh Hajibabzadeh, and Parviz Shahabi, "A New Brain-Robot Interface System Based on SVM-PSO Classifier," *2017 Artificial Intelligence and Signal Processing Conference (AISP)*, Shiraz, Iran, pp. 124-128, 2017. [CrossRef] [Google Scholar] [Publisher Link]

[34] V. Muthuvel Vijai, and P. A. Mathina, "An Effective Ring Partition and Half Toning Combined Face Morphing Detection," *International Journal of Computer and Organization Trends*, vol. 11, no. 4, pp. 10-14, 2021. [CrossRef] [Publisher Link]

[35] S. Ramesh, and D. Vydeki, "Recognition and Classification of Paddy Leaf Diseases using Optimized Deep Neural Network with Jaya Algorithm," *Information Processing in Agriculture*, vol. 7, no. 2, pp. 249-260, 2019. [CrossRef] [Google Scholar] [Publisher Link]

[36] Xuchun Li, Lei Wang, and Eric Sung, "AdaBoost with SVM-Based Component Classifiers," *Engineering Applications of Artificial Intelligence*, vol. 21, no. 5, pp. 785-795, 2008. [CrossRef] [Google Scholar] [Publisher Link]

[37] M. Rajababu, K. Srinivas, and H. Ravisankar, "MF-FaceNet: An Intuitive Age-Invariant Face Recognition through Multi-Feature and Multi-Fusion CNNs," *International Journal of Engineering Trends and Technology*, vol. 71, no. 3, pp. 407-422, 2023. [CrossRef] [Publisher Link]

[38] Gaurav Agarwal, and Hari Om, "Performance of Deer Hunting Optimization Based Deep Learning Algorithm for Speech Emotion Recognition," *Multimedia Tools and Applications*, vol. 80, pp. 9961-9992, 2021. [CrossRef] [Google Scholar] [Publisher Link]

[39] Benyamin Abdollahzadeh, Farhad Soleimanian Gharehchopogh, and Seyedali Mirjalili, "African Vultures Optimization Algorithm: A New Nature-Inspired Metaheuristic Algorithm for Global Optimization Problems," *Computers & Industrial Engineering*, vol. 158, p. 107408, 2021. [CrossRef] [Google Scholar] [Publisher Link]

[40] Mohd Herwan Sulaiman et al., "Barnacles Mating Optimizer: A New Bio-Inspired Algorithm for Solving Engineering Optimization Problems," *Engineering Applications of Artificial Intelligence*, vol. 87, p. 103330, 2020. [CrossRef] [Google Scholar] [Publisher Link]